

Search for Exoplanets around Northern Circumpolar Stars

V. Three likely planetary companions to the giant stars HD 19615, HD 150010, and HD 174205

G. Jeong (정광희)¹, B.-C. Lee (이병철)^{2,3}, M.-G. Park (박명구)⁴, T.-Y. Bang (방태양)⁴, and I. Han (한인우)²

¹ Antbridge Technology, 79-1, 101 Gajeong-ro Yuseong-gu, Daejeon 34120, Korea
e-mail: tlotv1@gmail.com

² Korea Astronomy and Space Science Institute, 776, Daedeokdae-Ro, Yuseong-Gu, Daejeon 34055, Korea
e-mail: [bcLee; iwhan]@kasi.re.kr

³ Korea University of Science and Technology, Gajeong-ro Yuseong-gu, Daejeon 34113, Korea

⁴ Department of Astronomy and Atmospheric Sciences, Kyungpook National University, Daegu 41566, Korea
e-mail: mgp@knu.ac.kr; apollo.choe@gmail.com

Received October 6, 2021; accepted November 9, 2021

ABSTRACT

Aims. We report the detection of long-period radial velocity (RV) variations in three giant stars, HD 19615, HD 150010, and HD 174205, using precise RV measurements.

Methods. These detections are part of the Search for Exoplanets around Northern Circumpolar Stars (SENS) survey being conducted at the Bohyunsan Optical Astronomy Observatory (BOAO). The nature of the RV variations was investigated by analyzing the photometric and line shape variations. We found no variability with the RV period in these quantities and conclude that the RV variations are most likely caused by planetary companions.

Results. Orbital solutions for the three stars yield orbital periods of 402 d, 562 d, and 582 d and minimum masses of $8.5 M_J$, $2.4 M_J$, and $4.2 M_J$, respectively. These masses and periods are typical for planets around intermediate-mass stars, although some unclear interpretations and recent studies may be calling some planet convictions into question. Nevertheless, the SENS program is contributing to our knowledge of giant planets around intermediate-mass stars.

Key words. stars: individual: HD 19615, HD 150010, and HD 174205 — stars: planetary systems — techniques: radial velocities

1. Introduction

The measurements of stellar radial velocity (RV) are one of the most successful techniques employed in the search for exoplanets. We have been conducting an exoplanet search program around late-type giant stars since 2004. This program has made substantial contributions to both exoplanet and asteroseismic studies around giant stars (Han et al. 2010; Lee et al. 2011, 2012a,b, 2013, 2014a,b). However, these works were occasionally hampered by an aliasing effect caused by the seasonal dependence of observations. To cope with this bias, we started the Search for Exoplanets around Northern Circumpolar Stars (SENS; Lee et al. 2015) survey in 2010. Because all targets of the SENS program can be observed during all seasons throughout the year, the seasonal bias is minimized. Furthermore, this strategy improved the observation efficiency by reducing the telescope slew time. (Lee et al. 2012a)

Here we present the detection of three new planet candidates. Section 2 introduces the observation strategy. The stellar properties and the analyses are described in detail in Sect. 3. We report the analyses of RV variations and the results of the measurements in Sect. 4, and, finally, our discussion of the results is presented in Sect. 5.

2. Observations

Since January 2010, we have collected a total of 52, 54, and 57 spectral data points for HD 19615, HD 150010, and HD 174205, respectively. The three stars were observed with the high-resolution fiber-fed Bohyunsan Observatory Echelle Spectrograph (BOES; Kim et al. 2007) of the 1.8 m telescope at Bohyunsan Optical Astronomy Observatory (BOAO). Because the candidates are concentrated around the pole star, observations are possible throughout the year. Thus, the SENS survey has an advantage in terms of period coverage. For precise RV measurements, an iodine absorption (I_2) cell was placed in the optical path in front of the fiber entrance (Han et al. 2007). This is based on the method by Valenti et al. (1995) and Butler et al. (1996). We also used the matrix formula described by Endl et al. (2000) for the modeling of the instrument profile. And using singular value decomposition instead of the maximum entropy method adopted by Endl et al. (2000), we solved the matrix equation.

The target stars have a V-magnitude range of 6.4–6.7, and we adopted a 200 μm fiber, an adequate trade-off between the optical efficiency and fiber resolution, which provides a spectral resolution of 45,000. The typical exposure time is limited to less than 20 minutes, which yields a signal-to-noise ratio of about 150. In order to check the instrumental stability, we have monitored an RV standard star, τ Ceti, since 2003. The long-term RV

Table 1. RV measurements for HD 19615 from February 2010 to March 2021 using the BOES.

JD -2,450,000	RV m s ⁻¹	$\pm\sigma$ m s ⁻¹	JD -2,450,000	RV m s ⁻¹	$\pm\sigma$ m s ⁻¹	JD -2,450,000	RV m s ⁻¹	$\pm\sigma$ m s ⁻¹
5250.122138	172.1	13.9	7327.282286	375.8	11.7	8932.016082	297.0	18.9
5842.239861	-135.9	10.4	7704.032537	419.6	12.1	8933.033641	331.2	26.2
5933.110447	-269.3	13.1	7757.119503	90.8	10.8	8942.963325	198.6	15.7
5962.989966	-192.3	12.3	7758.088199	34.1	13.8	8945.014470	201.6	17.1
6259.132566	-256.3	10.0	7813.013370	-62.4	11.5	8969.961480	178.8	19.5
6287.044466	-293.7	18.5	7855.011677	-81.4	22.9	9149.317839	-168.9	12.2
6288.161790	-166.4	9.5	7855.986123	-155.7	15.2	9150.041118	-190.8	21.3
6347.047078	-101.5	12.9	8015.212962	48.9	11.8	9151.008641	-184.4	11.1
6551.243387	133.2	11.9	8092.145036	174.8	13.6	9161.097381	-177.0	12.6
6578.277410	-13.3	14.4	8109.225577	90.8	12.8	9161.108724	-148.6	12.8
6617.007990	-98.8	9.5	8516.945624	88.1	12.0	9161.097381	-177.0	12.6
6714.072126	-109.5	17.3	8561.987563	-13.2	15.0	9161.108724	-148.6	12.8
6739.961457	-120.5	10.6	8830.238542	-78.7	17.6	9162.194690	-141.3	13.0
6808.255282	-147.6	20.5	8849.167430	121.2	41.3	9217.071292	-132.7	15.4
6922.137214	106.6	11.8	8852.045193	49.0	14.2	9218.071261	-167.9	15.0
6965.371019	234.8	12.4	8862.029439	117.6	13.6	9298.983663	30.0	15.2
7094.012094	-227.1	12.9	8863.129164	161.4	16.5			
7298.026234	410.2	10.7	8893.969101	201.4	16.5			

Table 2. RV measurements for HD 150010 from June 2010 to June 2021 using the BOES.

JD -2,450,000	RV m s ⁻¹	$\pm\sigma$ m s ⁻¹	JD -2,450,000	RV m s ⁻¹	$\pm\sigma$ m s ⁻¹	JD -2,450,000	RV m s ⁻¹	$\pm\sigma$ m s ⁻¹
5357.027343	11.3	18.6	7475.184243	-14.8	17.4	8943.045719	35.5	16.9
5616.392269	143.6	25.1	7527.109889	-40.3	17.5	8943.066656	25.6	15.9
5671.011796	163.2	24.4	7530.213694	-19.7	19.3	8944.157323	54.2	19.0
5842.957103	4.6	20.8	7704.941274	19.5	14.1	8945.081580	77.2	16.9
6379.262625	51.6	14.6	7819.259376	9.2	15.0	8969.097550	23.8	18.2
6409.327670	-1.2	14.6	7856.248364	-18.3	15.2	8970.135878	18.2	17.5
6583.040523	60.6	25.3	7895.087187	-46.2	16.7	9008.990863	77.3	22.6
6710.321857	99.2	15.0	8010.998230	-58.6	13.2	9128.930702	-2.4	16.6
6739.165553	46.3	15.1	8037.017169	-84.1	18.4	9148.968556	-37.8	12.4
6805.184754	42.4	18.1	8105.359985	-47.5	15.2	9149.918236	-51.0	14.6
6921.965641	-102.7	16.2	8743.003171	-103.8	14.7	9150.910347	-53.3	13.5
6963.939995	-36.9	19.6	8772.957082	-32.9	13.7	9160.945100	-74.0	19.0
6970.901351	-80.4	15.8	8852.378263	11.7	17.2	9161.952258	-54.6	15.9
7027.383448	-73.2	16.5	8863.303083	-49.7	17.0	9296.119476	-75.0	20.6
7067.324662	-20.2	20.7	8898.199527	6.9	21.4	9330.007068	-81.1	61.1
7148.089384	-8.5	17.7	8927.267737	4.0	20.0	9359.173258	10.2	20.4
7169.267191	86.2	18.3	8932.072411	56.9	22.5	9370.048097	51.5	44.1
7298.972916	8.8	15.2	8933.077617	80.6	23.7	9370.173096	-13.0	16.5

stability of the BOES was ~ 7 m s⁻¹ (Lee et al. 2013). The RV measurements are listed in Tables 1-3.

3. Stellar properties

We adopted the basic stellar parameters (spectral type, visual magnitude, B-V color index, and RV) from the *HIPPAR-COS* catalog (ESA 1997) and Anderson & Francis (2012). To use more recent effective temperature, parallax, and luminosity data, photometry parameters from Gaia Data Release 2 (DR2; Gaia Collaboration et al. 2018) were obtained.

We determined the effective temperature and surface gravity with the measured equivalent widths of Fe I and Fe II lines of each stellar spectrum (Takeda et al. 2002). The surface gravity was determined from the ionization equilibrium of Fe I and Fe II. The metallicity ([Fe/H]) and microturbulent velocity

(v_{micro}), including T_{eff} and $\log g$, were derived from the TGVIT code (Takeda et al. 2005).

The stellar age, radius, and mass for each star were calculated using the online tool PARAM 1.3¹ (da Silva et al. 2006) for given parameters T_{eff} , [Fe/H], m_v , and π . This tool is based on a library of theoretical stellar isochrones (Girardi et al. 2000; Bressan et al. 2012) and the Bayesian estimation method (Jørgensen & Lindegren 2005).

Generally, in evolved stars, the low-amplitude, long-period RV variations can originate from the rotational modulation of the surface with inhomogeneities. We estimated the stellar rotational velocities using the line broadening technique (Takeda et al. 2008). The stellar parameters of the observed stars are summarized in Table 4.

¹ http://stev.oapd.inaf.it/cgi-bin/param_1.3/

Table 3. RV measurements for HD 174205 from February 2010 to June 2021 using the BOES.

JD	RV	$\pm\sigma$	JD	RV	$\pm\sigma$	JD	RV	$\pm\sigma$
-2,450,000	m s^{-1}	m s^{-1}	-2,450,000	m s^{-1}	m s^{-1}	-2,450,000	m s^{-1}	m s^{-1}
5248.349219	76.0	9.3	7703.935737	33.9	8.2	8933.159881	103.4	12.1
5456.162247	13.0	7.4	7705.013445	44.3	7.7	8943.148932	31.1	9.5
5672.200478	-67.8	11.4	7756.929401	42.4	8.7	8943.164175	39.1	9.5
5844.052953	19.8	9.0	7757.942321	60.4	11.8	8944.179621	84.1	12.5
6287.934421	-71.1	8.7	7856.322146	15.5	9.6	8944.194933	92.4	10.4
6410.265546	7.5	8.5	7893.146122	-25.4	8.9	8945.143700	69.8	9.0
6681.350238	36.5	10.6	7934.189754	-4.9	9.0	8969.130023	41.5	11.4
6739.189411	59.9	11.8	8015.076632	-99.0	7.8	8970.154940	96.6	11.2
6805.230356	24.3	10.6	8091.946858	-60.9	11.5	9128.947432	-42.3	9.1
6921.989868	-45.8	8.7	8109.912914	-11.3	9.0	9148.987572	-29.7	10.7
6967.945510	-88.8	8.0	8743.048983	31.0	7.6	9149.969785	-33.4	8.5
7066.310819	-93.7	14.4	8772.993155	27.0	8.7	9150.957381	-8.6	9.8
7068.260174	-61.8	10.1	8826.877616	24.2	9.2	9152.007233	-90.8	8.8
7148.147847	4.3	10.9	8829.916120	24.1	9.6	9160.973048	-66.7	10.3
7171.236702	32.3	9.5	8831.904548	33.7	11.2	9160.987955	-75.4	8.9
7299.018323	0.6	11.7	8852.388466	-16.7	11.9	9161.975479	3.9	10.7
7475.271895	-139.2	10.7	8863.322980	48.8	14.3	9296.267940	-24.6	11.1
7525.170621	-125.0	7.2	8898.315208	46.5	13.1	9359.214704	6.6	12.6
7530.266309	-94.9	8.6	8933.146224	73.4	13.5	9370.212997	29.1	9.0

Table 4. Stellar parameters for the stars analyzed in the present paper.

Parameter	HD 19615	HD 150010	HD 174205	Ref.
Spectral type	K0	K2 III	K2	1
m_v (mag)	6.697 ± 0.001	6.427 ± 0.001	6.444 ± 0.001	1
$B-V$ (mag)	1.465 ± 0.008	1.291 ± 0.008	1.234 ± 0.007	1
RV (km s^{-1})	-35.21 ± 0.20	-35.81 ± 0.21	-5.41 ± 0.20	1
π (mas)	3.74 ± 0.03	6.89 ± 0.03	4.24 ± 0.03	2
T_{eff} (K)	3987 ± 125	4256 ± 125	4393 ± 125	2
	4263 ± 38	4153 ± 83	4308 ± 25	3
[Fe/H]	-0.31 ± 0.11	-0.25 ± 0.22	-0.28 ± 0.33	3
$\log g$ (cgs)	1.4 ± 0.1	2.1 ± 0.1	1.8 ± 0.1	3
v_{micro} (km s^{-1})	1.85 ± 0.12	1.27 ± 0.10	1.49 ± 0.08	3
Age (Gyr)	6.7 ± 1.8	4.9 ± 1.1	1.7 ± 0.3	3
R_{\star} (R_{\odot})	32.3 ± 0.9	16.2 ± 0.4	26.6 ± 0.6	3
M_{\star} (M_{\odot})	1.1 ± 0.1	1.3 ± 0.1	1.8 ± 0.1	3
L_{\star} (L_{\odot})	327 ± 3	96 ± 1	239 ± 2	2
$v_{\text{rot}} \sin i$ (km s^{-1})	2.6 ± 0.5	2.2 ± 0.5	1.6 ± 0.5	3
$P_{\text{rot}} / \sin i$ (days)	560	391	866	3

References.— (1) Anderson & Francis (2012); (2) Gaia Collaboration et al. (2018); (3) This work.

4. Orbital solutions

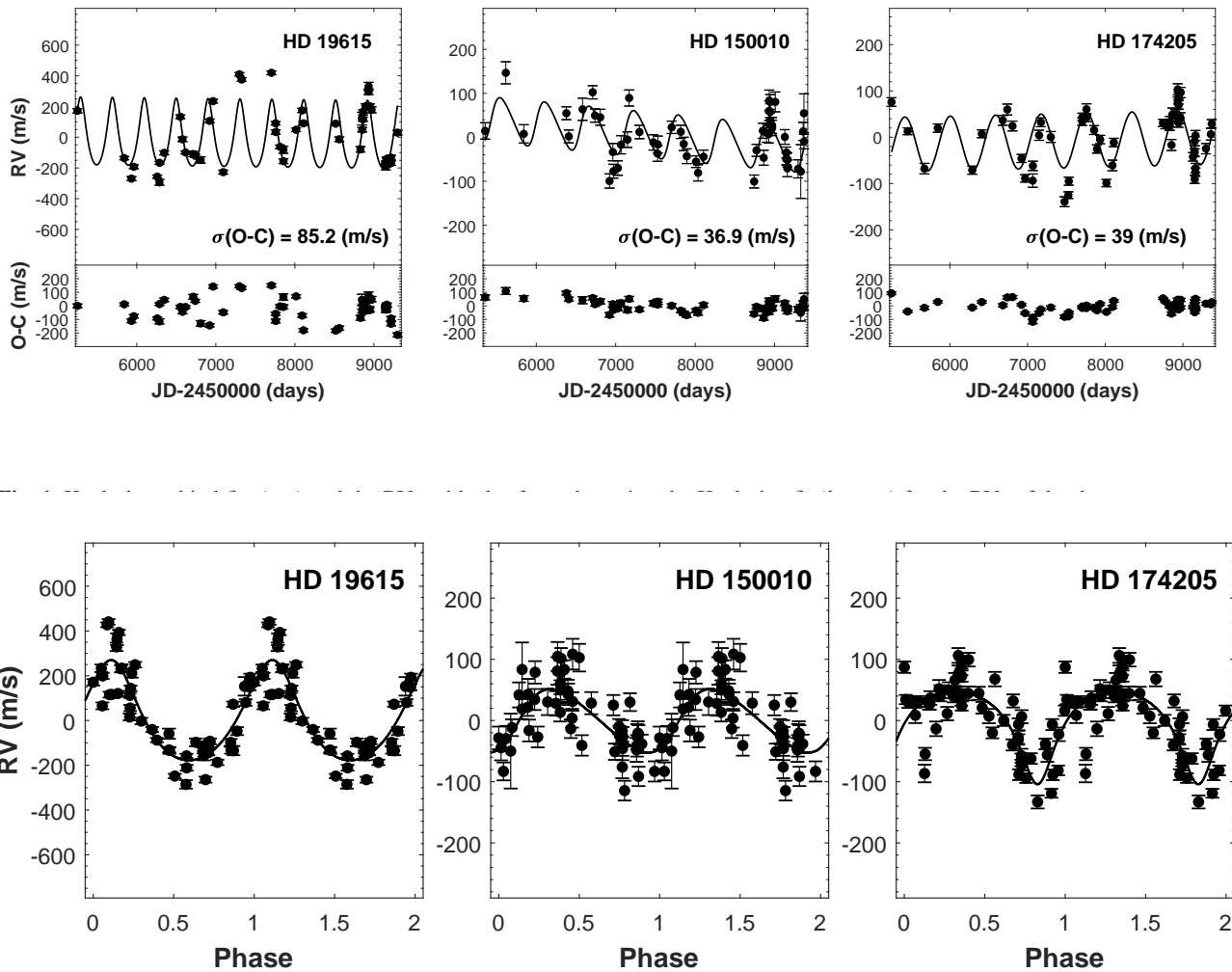
We obtained three targets spanning 11 years, which show clear periodic variations. Initial values for the period were determined via Lomb-Scargle (L-S) analysis, which is appropriate for long-period variations with long-term sporadic observations (Lomb 1976; Scargle 1982). From this initial period, we determined all the orbital elements via fitting with Keplerian orbit models in the *Systemic Console 2* (Meschiari et al. 2009). We applied the same method to the three stars to find the best-fit Keplerian orbital motion for the observed RV variations. We estimated the parameter uncertainties using the bootstrap routine within *Systemic Console 2* with 10,000 synthetic data set realizations. The orbital parameters are listed in Table 5.

The RV data of the three stars are plotted over six cycles along with the best Keplerian orbital fit in the upper panels of Fig. 1. As can be seen from the bottom panel of Fig. 1, most of the rms of the RV residuals are significantly larger than the

long-term uncertainty measured by the observation of the RV standard star, $\sim 7 \text{ m s}^{-1}$, and the typical internal error of individual RV precisions, $\sim 13 \text{ m s}^{-1}$, and they are consistent with the expected RV scatter (so-called jitter) in giants. Yet they do not show any systemic pattern. These residuals are probably from typical intrinsic RV variations in K giant stars (Sato et al. 2005; Hekker et al. 2006). Furthermore, all of the target stars show a slight linear trend, which may have been caused by an unseen distant companion. The long-term linear trend is indeed significant and could be caused by a distant companion. Horch et al. (2012) reported a distant binary companion to HD 150010 with speckle interferometry, at a projected separation of 1 arcsecond. This companion may possibly be the source of the long-term linear RV trend. Figure 2 shows the RV measurements phased to the orbital periods for all stars.

Table 5. Orbital parameters for the companions.

Parameter	HD 19615 b	HD 150010 b	HD 174205 b
P (days)	402 ± 2	562 ± 8	582 ± 17
K (m s^{-1})	224 ± 18	52 ± 8	76 ± 11
$T_{\text{periastron}}$ (JD)	2449662 ± 91	2449811 ± 175	2449918 ± 197
e	0.2 ± 0.1	0.2 ± 0.1	0.4 ± 0.2
ω (deg)	279 ± 71	137 ± 91	94 ± 93
$m \sin i$ (M_J)	8.5 ± 0.7	2.4 ± 0.4	4.2 ± 0.5
a (AU)	1.1 ± 0.1	1.4 ± 0.1	1.7 ± 0.1
$Slope$ ($\text{m s}^{-1}\text{yr}^{-1}$)	-9 ± 10	-20 ± 5	2 ± 4
N_{obs}	52	54	57
RMS (m s^{-1})	85.2	36.9	39

**Fig. 2.** Phase-folded RV curves of the three stars.

5. Stellar activity and pulsation diagnostics

The periodic variations of RVs can also be caused by some intrinsic activities of the stars, such as chromospheric activity, stellar pulsation, and rotational modulation of the surface feature. In order to identify the nature of the RV variations, we investigated Ca II H lines, photometric data, and spectral line profile variations.

5.1. Photometric variations

The photometric data of *HIPPARCOS* for our three target stars were obtained between November 1989 and March 1993. They are not contemporaneous with more recent BOES RV measurements. However, because photometric data cover the time interval relevant to a maximum period of 1071 days in our study, an examination of the *HIPPARCOS* photometry may reveal periodic variations, possibly caused by rotational modulation of surface features or stellar oscillations. We thus used a total of

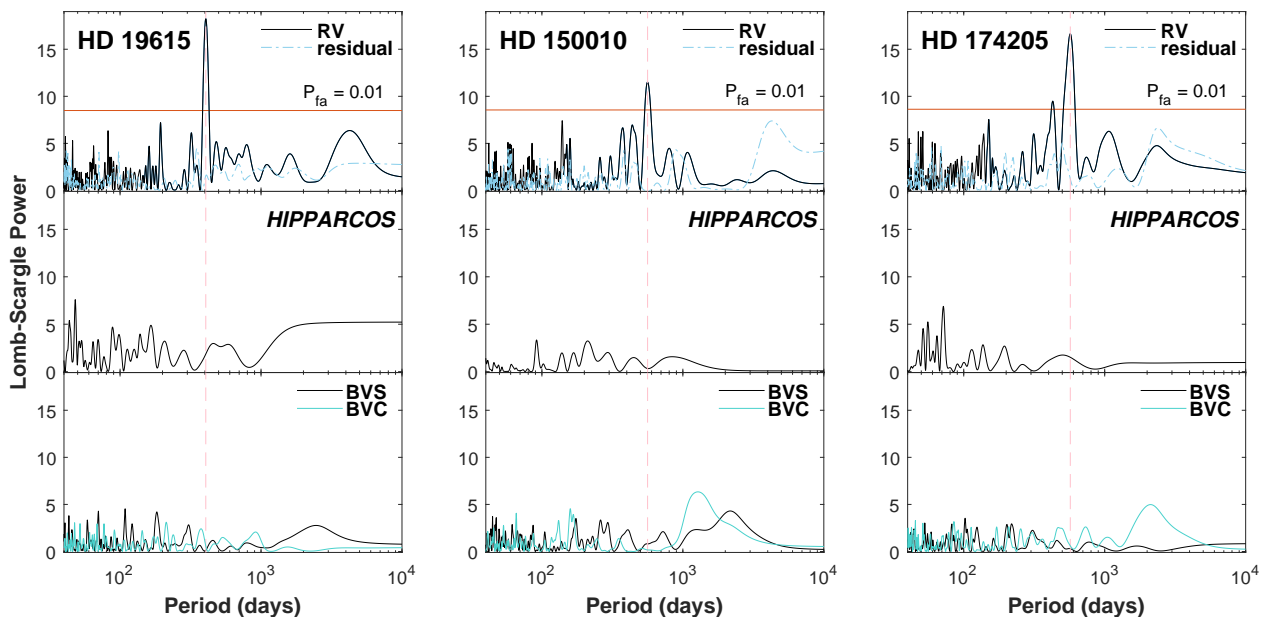


Fig. 3. L-S periodograms of the RV measurements and residuals (*top*), *HIPPARCOS* photometry (*middle*), and the line bisectors of the span and curvature (*bottom*) for the three stars. The vertical dashed lines indicate the periods of each star.

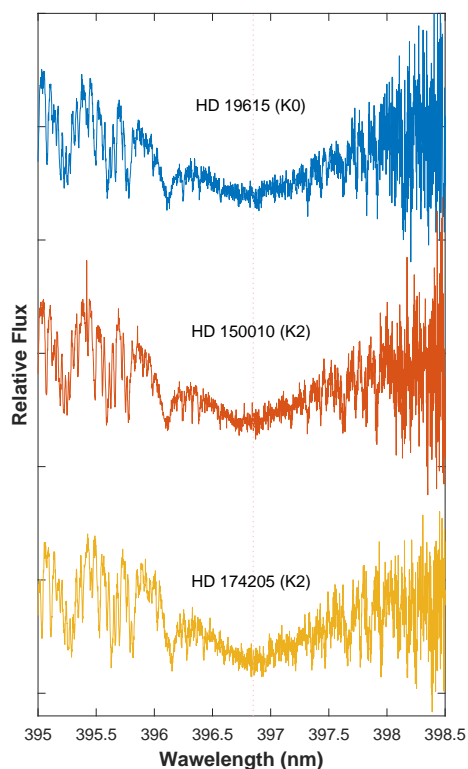


Fig. 4. Spectra in the region of the Ca II H line. The vertical dotted line marks the center of the Ca II H profiles (3968.5 Å).

160, 143, and 119 observations of HD 19615, HD 150010, and HD 174205, respectively.

The rms scatters are 0.011, 0.007, and 0.011 mag for the three stars, respectively, which were comparable to the photometric uncertainties of *HIPPARCOS* data. We also analyzed the L-S periodogram with photometric data and could not find any

periodicity corresponding to the RV variations (middle panels in Fig. 3).

5.2. Line bisector variations

An examination of spectral line shapes has become an important tool in identifying the origin of RV variations (Hatzes & Cochran 1998). Whereas the orbital motion by a companion causes a Doppler shift without a change in the line shape, rotational modulation of stellar surface structures gives rise to RV variations accompanied by line shape variations. We thus investigated the change in the shapes of spectral lines using two bisectors: the bisector velocity span (BVS), the difference in velocity between the 0.8 and 0.4 flux levels of the continuum value, and the bisector velocity curvature (BVC), the difference in the velocity span of the upper and lower half of the bisector.

In order to avoid contaminations from other spectral lines, I_2 absorption lines, and telluric absorption lines, we selected the lines in the spectral region 6000Å – 6800Å. The selected lines, such as Fe, Mn, Ti, Ni, and Cr lines, were relatively deep under the 0.3 intensity level of the continuum value. We chose different lines for each star depending on the spectral type. Finally, we obtained the average bisector value by combining individual bisector measurements. The L-S periodograms of the bisectors, both BVS and BVC, do not show any significant peaks associated with those of the RV variations (bottom panels in Fig 3).

5.3. Pulsations

All target stars are evolved stars that are classified as K0, K2, or K2. Because most K giant stars have intrinsic mechanisms that may produce periodic RV variations, possible mechanisms such as pulsations should be investigated carefully (Hekker et al. 2008). Some K giant stars are known to be pulsating stars, which usually pulsate on several modes. Taking into account the K0-M3 classification and surface gravity of our stars, we can exclude

known types of pulsations as the origin of the observed RV variations. The reason is that RV detected periods are much longer than the expected fundamental radial mode pulsations. The non-radial modes are more difficult to identify than the radial modes. We thus have to wait for a more detailed understanding of the new forms of oscillations that can be rotated to very long period oscillations (on the order of several years).

5.4. Surface activity

A rotating star with surface features such as spots caused by chromospheric activity may exhibit periodic RV variations, which can be misinterpreted as a planetary signal (Queloz et al. 2001). The Ca II H line (3968.5 Å) has traditionally been used as an indicator of stellar activity (Eberhard & Schwarzschild 1913). If there is chromospheric activity, an emission line will be shown at the center of the Ca II H absorption line profile. Several evolutionary stages of chromospheric activity surveyed recently around late-type evolved stars (Setiawan et al. 2005; Meszaros et al. 2008; Mészáros et al. 2009) have allowed us to investigate the oscillation of the magnetic activity of late-type giant stars. We plotted the Ca II H line of each star in Fig. 4. There are no noteworthy emissions at the core of Ca II H lines for any of the target stars. Considering all the facts, we conclude that the regular RV variations in our target stars are most likely caused by orbiting planetary companions.

6. Discussion

We have detected long-period RV variations in three giant stars. The stars show no variations in line shape as measured by the spectral line bisectors. Our target stars also seem to show a lack of variations in the *HIPPARCOS* photometry. However, the lack of photometric variations is only suggestive as the *HIPPARCOS* measurements were not contemporaneous to our data.

Although the exact nature of long-secondary periods (LSPs) in giants is still unknown, Wood et al. (2004) speculated that the origin of long-period RV variations for LSP giants can be explained as a non-radial pulsation in a low-degree g^+ mode with star spot activities. Saio et al. (2015) also suggested that the length of the LSPs was roughly consistent with the periods predicted from the non-radial pulsation in the oscillatory convective mode, which is a g^- mode in a strongly non-adiabatic condition. However, the photometric variation for the stars may not be related to this mechanism, which operates in LSP giants. Also, the amplitudes of RV variations are much smaller than those of typical LSPs.

Hatzes et al. (2018) and Reichert et al. (2019) both found RV signals that masqueraded as planetary companions with periods of a few hundred days and masses of a few Jovian masses around the K5 giants Gamma Draconis and Aldebaran. They concluded that the most likely cause seems to be a type of stellar oscillation in evolved K giants. Thus, further investigation into the origin of giant stars is needed before conclusions on the true cause of the RV variations in giant stars can be made.

On the other hand, Döllinger & Hartmann (2021) showed that planet discoveries around stars with radii larger than $21 R_{\odot}$ seem to be rather problematic (this applies to HD 19615 and HD 174205, while HD 150010 is slightly below this radius limit). Many of the stars with questionable planets have $[Fe/H] < 0$, which applies to all three stars of the current sample. Finally, all these spurious planets have periods in the range between 300 and 800 days, which again applies to all three stars. Stars with

the given properties seem to show intrinsic RV variations of a so far unknown mechanism, which makes them very problematic targets for a planet search via the Doppler method.

Despite the possible verification of the cause of the long-term RV variations in giant stars at this point, the result of our research may be somewhat negative in light of recent research (Döllinger & Hartmann 2021). Therefore, it is necessary to develop a new, improved interpretation method in the future.

Based on measurements conducted by Kervella et al. (2019) of the proper motion anomaly between *HIPPARCOS* and *Gaia* DR2 main astrometry, the astrometric detection limits at 1 AU from this paper for HD 16915, HD 150010, and HD 174205 are $\sim 5M_J$, $\sim 3.2M_J$, and $\sim 1.4M_J$, respectively. Of course, these are slightly below or above the reported RV minimal masses of the companions. The future *Gaia* DR4 astrometry will be even more detailed and precise.

Acknowledgements. BCL acknowledges partial support by the KASI (Korea Astronomy and Space Science Institute) grant 2021-1-830-08 and acknowledge support by the National Research Foundation of Korea(NRF) grant funded by the Korea government(MSIT) (No.2021283200). M.G.P. was supported by the Basic Science Research Program through the National Research Foundation of Korea (NRF) funded by the Ministry of Education (2019R111A3A02062242) and KASI under the R&D program supervised by the Ministry of Science, ICT and Future Planning. This research made use of the SIMBAD database, operated at the CDS, Strasbourg, France.

References

- Anderson, E. & Francis, C. 2012, *Astronomy Letters*, 38, 331.
 Bressan, A., Marigo, P., Girardi, L., et al. 2012, *MNRAS*, 427, 127.
 Butler, R. P., Marcy, G. W., Williams, E., et al. 1996, *PASP*, 108, 500.
 Eberhard, G. & Schwarzschild, K. 1913, *ApJ*, 38, 292.
 da Silva, L., Girardi, L., Pasquini, L., et al. 2006, *A&A*, 458, 609.
 Döllinger, M. P. & Hartmann, M. 2021, *ApJS*, 256, 10.
 Endl, M., Kürster, M., & Els, S. 2000, *A&A*, 362, 585.
 ESA, . 1997 . 1997, *VizieR Online Data Catalog*, I/239
 Gaia Collaboration, Brown, A. G. A., Vallenari, A., et al. 2018, *A&A*, 616, A1.
 Girardi, L., Bressan, A., Bertelli, G., et al. 2000, *A&AS*, 141, 371.
 Han, I., Kim, K.-M., Byeong-Cheol, L., et al. 2007, *Publication of Korean Astronomical Society*, 22, 75.
 Han, I., Lee, B. C., Kim, K. M., et al. 2010, *A&A*, 509, A24.
 Hatzes, A. P. & Cochran, W. D. 1998, *Cool Stars, Stellar Systems, and the Sun*, 154, 311
 Hatzes, A. P., Endl, M., Cochran, W. D., et al. 2018, *AJ*, 155, 120.
 Hekker, S., Reffert, S., Quirrenbach, A., et al. 2006, *A&A*, 454, 943.
 Hekker, S., Snellen, I. A. G., Aerts, C., et al. 2008, *A&A*, 480, 215.
 Horch, E. P., Howell, S. B., Everett, M. E., et al. 2012, *AJ*, 144, 165.
 Jørgensen, B. R. & Lindegren, L. 2005, *A&A*, 436, 127.
 Kervella, P., Arenou, F., Mignard, F., et al. 2019, *A&A*, 623, A72.
 Kim, K.-M., Han, I., Valyavin, G. G., et al. 2007, *PASP*, 119, 1052.
 Lee, B.-C., Mkrtichian, D. E., Han, I., et al. 2011, *A&A*, 529, A134.
 Lee, B.-C., Han, I., Park, M.-G., et al. 2012a, *A&A*, 546, A5.
 Lee, B.-C., Mkrtichian, D. E., Han, I., et al. 2012b, *A&A*, 548, A118.
 Lee, B.-C., Han, I., & Park, M.-G. 2013, *A&A*, 549, A2.
 Lee, B.-C., Han, I., Park, M.-G., et al. 2014a, *A&A*, 566, A67.
 Lee, B.-C., Han, I., Park, M.-G., et al. 2014b, *JKAS*, 47, 69.
 Lee, B.-C., Park, M.-G., Lee, S.-M., et al. 2015, *A&A*, 584, A79.
 Lomb, N. R. 1976, *Ap&SS*, 39, 447.
 Meschiri, S., Wolf, A. S., Rivera, E., et al. 2009, *PASP*, 121, 1016.
 Meszaros, S., Dupree, A. K., & Szentgyorgyi, A. 2008, *AJ*, 135, 1117.
 Mészáros, S., Dupree, A. K., & Szalai, T. 2009, *AJ*, 137, 4282.
 Queloz, D., Henry, G. W., Sivan, J. P., et al. 2001, *A&A*, 379, 279.
 Reichert, K., Reffert, S., Stock, S., et al. 2019, *A&A*, 625, A22.
 Saio, H., Wood, P. R., Takayama, M., et al. 2015, *MNRAS*, 452, 3863.
 Sato, B., Kambe, E., Takeda, Y., et al. 2005, *PASJ*, 57, 97.
 Seargle, J. D. 1982, *ApJ*, 263, 835.
 Setiawan, J., von der Lühse, O., Pasquini, L., et al. 2005, *13th Cambridge Workshop on Cool Stars, Stellar Systems and the Sun*, 560, 963
 Takeda, Y., Sato, B., Kambe, E., et al. 2002, *PASJ*, 54, 1041.
 Takeda, Y., Ohkubo, M., Sato, B., et al. 2005, *PASJ*, 57, 27.
 Takeda, Y., Sato, B., & Murata, D. 2008, *PASJ*, 60, 781.
 Valenti, J. A., Butler, R. P., & Marcy, G. W. 1995, *PASP*, 107, 966.
 Wood, P. R., Olivier, E. A., & Kawaler, S. D. 2004, *ApJ*, 604, 800.